Technical Report 1623
August 1993

Optical Properties of Chromium and Neodymium in Zirconium-Barium-Lanthanum-Aluminum Fluoride Glass

F. E. Hanson
H. H. Caspers

Technical Report 1623
August 1993

Optical Properties of Chromium and Neodymium in Zirconium-Barium-Lanthanum-Aluminum Fluoride Glass

F. E. Hanson
H. H. Caspers

NAVAL COMMAND, CONTROL AND OCEAN SURVEILLANCE CENTER
RDT&E DIVISION
San Diego, California 92152–5000

K. E. EVANS, CAPT, USN
Commanding Officer

R. T. SHEARER
Executive Director

ADMINISTRATIVE INFORMATION

This report describes efforts to further develop and characterize solid-state laser materials for potential Navy applications. The work was carried out by the Electro-Optic Systems & Technology Branch and the Solid State Electronics Division. This report covers work from October 1987 to September 1988 and was approved for publication 27 July 1993.

Released by
D. Gookin, Head
Electro-Optic Systems &
Technology Branch

Under authority of
C. E. Gibbens, Head
Satellite Communications
Division

ACKNOWLEDGMENTS

The authors would like to thank the NCCOSC RDT&E Division Program Director for Research for supporting this work. We appreciate the help of H. E. Rast for his assistance with some of the Judd-Ofelt calculations. We are also grateful to O. H. El Bayoumi and T. M. Roberts for providing us with various ZBLA materials.

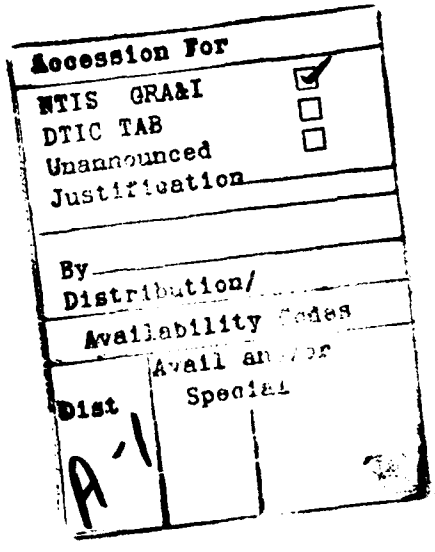

SM

CONTENTS

FIGURES

TABLES

INTRODUCTION

The heavy metal fluoride glasses are receiving a great deal of attention because of their potential use as fibers for infrared optical communication systems and as laser hosts for the development of visible and near-infrared lasers [1]. The transmission losses have resulted in the identification of $3d^n$ transition metal ion impurities incorporated during the growth of the heavy metal fluoride (HMF) glasses [2]. In these investigations, the $3d^n$ impurity centers were assumed to be in an O_h-type site symmetry and their energy levels identified with the aid of the Tanabe-Sugano energy diagrams [3]. To date, numerous investigations appear in the literature dealing with rare-earth impurity ions incorporated in HMF glasses [4]. The sensitization and energy transfer between sensitizer and acceptor impurity centers for the purpose of increasing the emission efficiency of the acceptor ion has become important in both glasses and single-crystal laser hosts [5].

In this report we describe the absorption and emission properties of Cr^{3+} and Cr^{3+},Nd^{3+} codoped zirconium-barium-lanthanum-aluminum (ZBLA) fluoride glass. Fluorescence decay curves are obtained over a range of temperatures. From the Nd^{3+}:ZBLA absorption spectrum the three phenomenological intensity parameters are calculated by using the Judd-Ofelt (JO) intensity model of electric-dipole transitions [6]. These parameters are compared with data obtained for Nd^{3+} in $Y_3Al_5O_{12}$, $Gd_3Sc_2Al_3O_{12}$, and LHG-8 glass. The calculated oscillator strengths for Nd:ZBLA agree well with the experimental values obtained from the absorption data.

EXPERIMENTAL

Samples used in this study were composed of 57 ZrF_4, 36 BaF_2, 3 LaF_3, (4-x) AlF3, x CrF_3, where x is equal to 0.25 and 0.5; and 57 ZrF_4, 36 BaF_2, (3-x) LaF_3, (4-y) AlF_3, x NdF_3, y CrF_3, where x is equal to 1 and 2, and y is equal to 0.25 and 0.5, respectively. The method for preparing the glass is described elsewhere [1]. The absorption spectra were recorded with a Varian 2390 spectrophotometer that operates from 200 to 3100 nm. A closed-cycle refrigerator system was used to obtain low-temperature absorption, emission, and decay rate measurements between 8 and 250 K. The fluorescence measurements were made by using short-pulse excitation from various dye lasers pumped with a pulsed YAG laser. The dyes of interest were pyridine, with emission at 670 nm, coumarin 460, and rhodamine, with their respective emissions at 460 and 580 nm. The fluorescent light was focused into a 0.5-m Jarrell-Ash spectrometer for spectral measurements or to isolate particular emission bands. Lifetimes were measured with an RCA 7102 S1 photomultiplier and a Tektronix 7912 programmable digitizer. Spectral measurements were made with an EG&G silicon reticon array, and the fluorescence intensities were corrected for instrument and detector response.

SPECTRAL CHARACTERISTICS OF Cr^{3+}:ZBLA

The room temperature and 8 K absorption measurements of 0.5 mole % Cr^{3+} in ZBLA are shown in figure 1. The spectrum of Cr^{3+} consists of two broad bands centered at 670 and 443 nm and assigned to the spin-allowed $^4A_2 - {}^4T_2$ and $^4A_2 - {}^4T_1$ electronic states of the octahedrally coordinated chromium ion [7]. The room temperature absorption band observed at 291 nm is assigned to the $^4A_2 - {}^4T_1$ transition. At 8 K, a very strong and sharp impurity band appears at 315 nm. Its temperature behavior and bandwidth is unlike any band associated with $3d^n$

transitions, either in amorphous or crystalline host materials. In some hosts, a charge transfer band at 370 nm has been observed and its properties shown to be associated with Cr^{6+} [8]. Our samples did not show any such extra absorption band. At 8 K, the broad long-wavelength absorption band at 670 nm shows three distinct subsidiary peaks. Their assignment has been the subject of some controversy. Following Lempicki et al. [9] in their study of Cr^{3+} in various glasses and of V^{2+}:KMgF3 by Sturge et al. [10], we interpret the "dips" in the 670 nm band as due to the interaction between the sharp ^2E and $^2T^1$ states with the vibrationally broadened $^4T_1$ quasicontinuum resulting in Fano antiresonances [11]. The assignments are indicated in figure 1 and the results summarized in table 1.

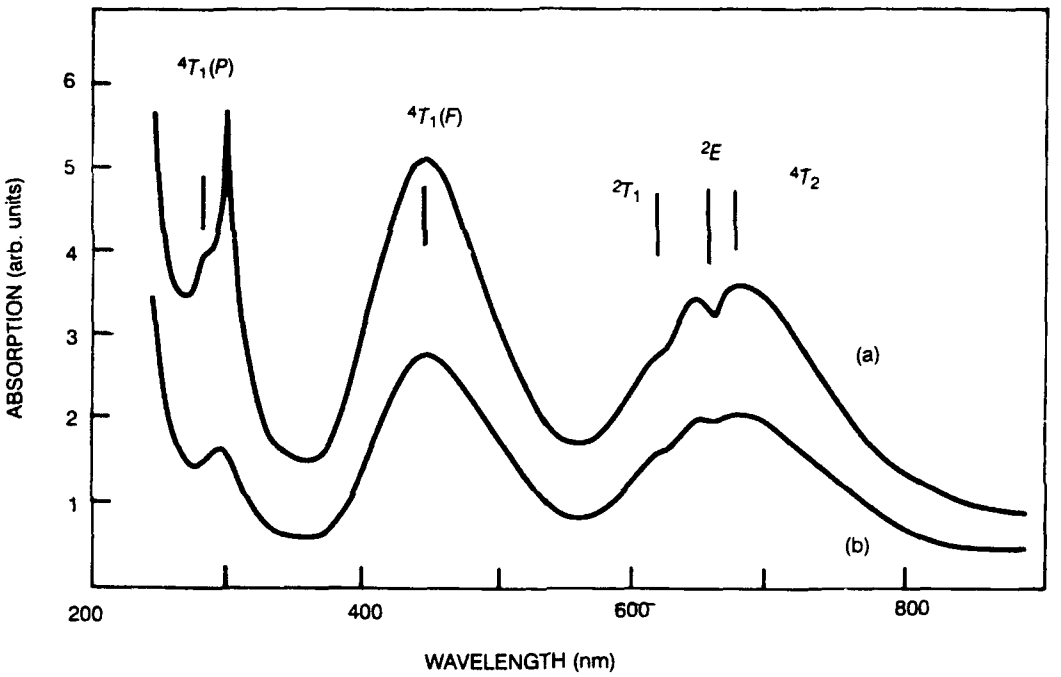

Figure 1. Absorption spectrum of Cr^{3+}:ZBLA at 8 K (a) and 300 K (b).

The ligand field parameter for Cr^{3+} in an octahedral site is determined directly from the $^4A_2 - {}^4T_2$ transition as $10\,D_q = 15040\ cm^{-1}$. The Racah parameter B, related to the interelectronic repulsion, can be determined from the relation

$$15B = \nu_3 + \nu_2 - 3\nu_1 \qquad (1)$$

Table 1. Assignments of chromium absorption bands.

Transition	λ (nm)	Assignment
$^4A_2 - {}^4T_2$	665	ν_1
$^4A_2 - {}^2E$	655	Spin Forbidden
$^4A_2 - {}^2T_1$	620	Spin Forbidden
$^4A_2 - {}^4T_1(F)$	443	ν_2
$^4A_2 - {}^4T_1(P)$	291	ν_3

From the assignments listed in table 1, B is found to be 790 cm^{-1}. This gives a value of 1.90 for the ratio Dq/B. Figure 2 shows the Tanabe-Sugano lower energy level diagram for octahedrally coordinated Cr^{3+}. The ratio Dq/B = 1.90 is indicated in figure 2. Broadband infrared emission centered at ~900 nm has been observed in various glasses [12]. It is attributed to the Stokes-shifted $^4T_2 - {}^4A_2$ fluorescence. Figure 3 shows the 8 K fluorescence using as excitation the emission of a pyridine dye laser at 670 nm. This allows us to pump directly into the $^4A_2 - {}^4T_2$ band of Cr^{3+}. Pumping into the higher $^4T_1$ band with a coumarin 460 dye laser gave identical results to the emission spectrum obtained by pumping into the $^4T_2$ band. We measured the fluorescence decay of the $^4T_2$ state at 900 nm over a range of temperatures, as shown in figure 4. The curves are nearly exponential, but there is some inhomogeneity due to the multitude of different Cr^{3+} ion sites and crystalline field environments in the glass. The strong quenching at higher temperature is evident. Above 250 K, the fluorescence intensity was too weak to obtain an adequate measurement. We define an integrated or average fluorescence lifetime, $\langle\tau\rangle$ according to

$$\langle\tau\rangle = \int_0^\infty I(t)dt/I(0) \tag{2}$$

where $I(t)$ is the shape of the decay curve. We also measured the incremental lifetimes, τ_1, at which the intensity decreased to $1/e$ of its initial value. For exponential decay, both of these measures are identical. Within experimental error, $\langle\tau\rangle$ was the same for laser excitation into either the $^4T_2$ or $^4T_1$ state, indicating a very rapid nonradiative transition from $^4T_1$ to $^4T_2$. The decay times $\langle\tau\rangle$ are plotted in figure 5 as a function of temperature. We note that τ_1 is generally less than $\langle\tau\rangle$ which is due to the inhomogeneous nature of the decay.

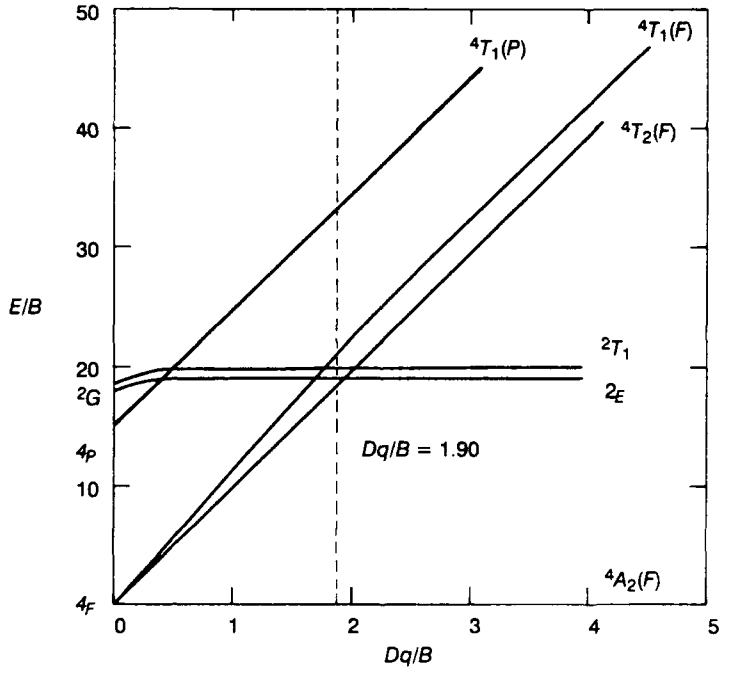

Figure 2. Lower energy levels versus crystal field strength in units of the Racah-parameter B for octahedrally coordinated Cr^{3+}.

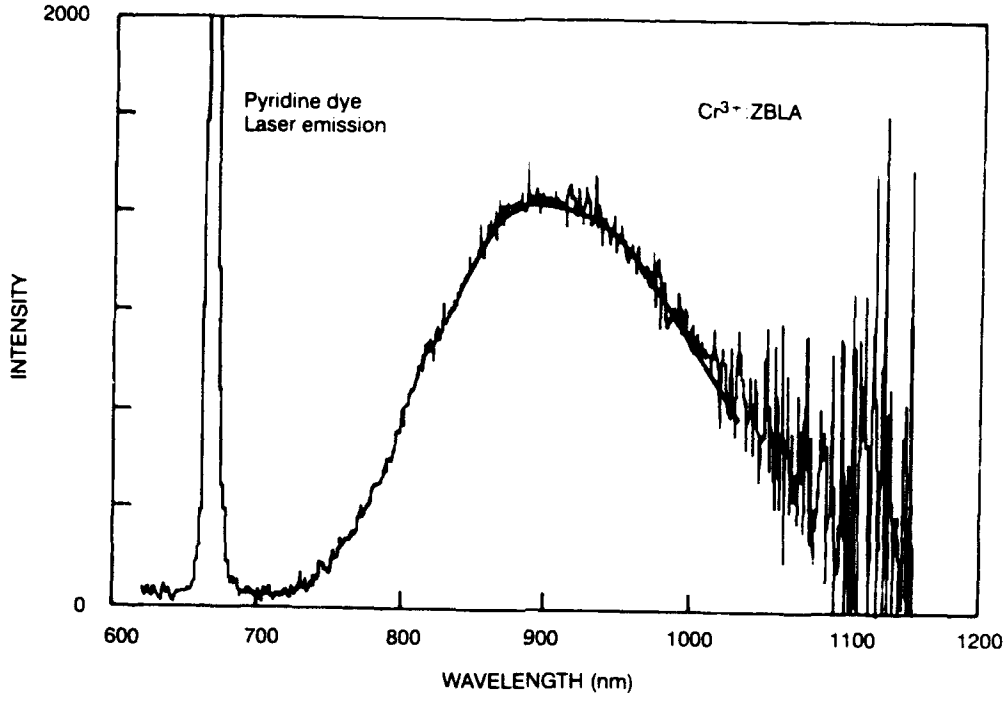

Figure 3. Fluorescence spectrum of Cr^{3+}:ZBLA at 8 K with pulsed excitation at 670 nm.

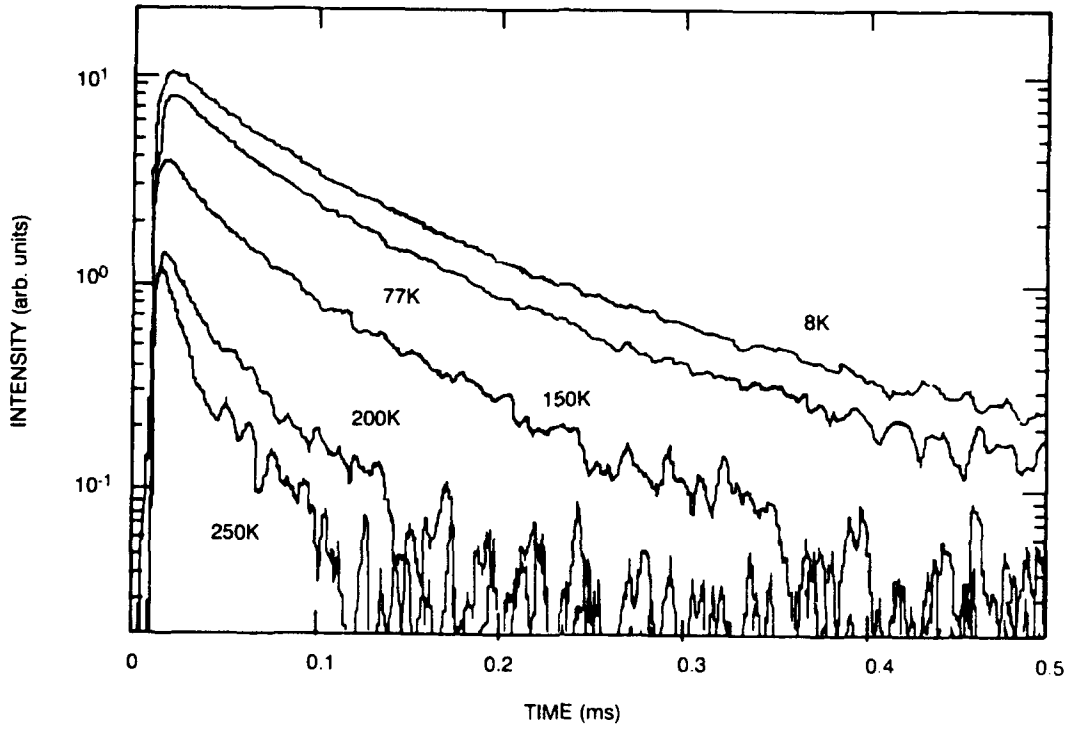

Figure 4. Fluorescence decay curves of Cr^{3+}:ZBLA glass at 900 nm with excitation at 670 nm.

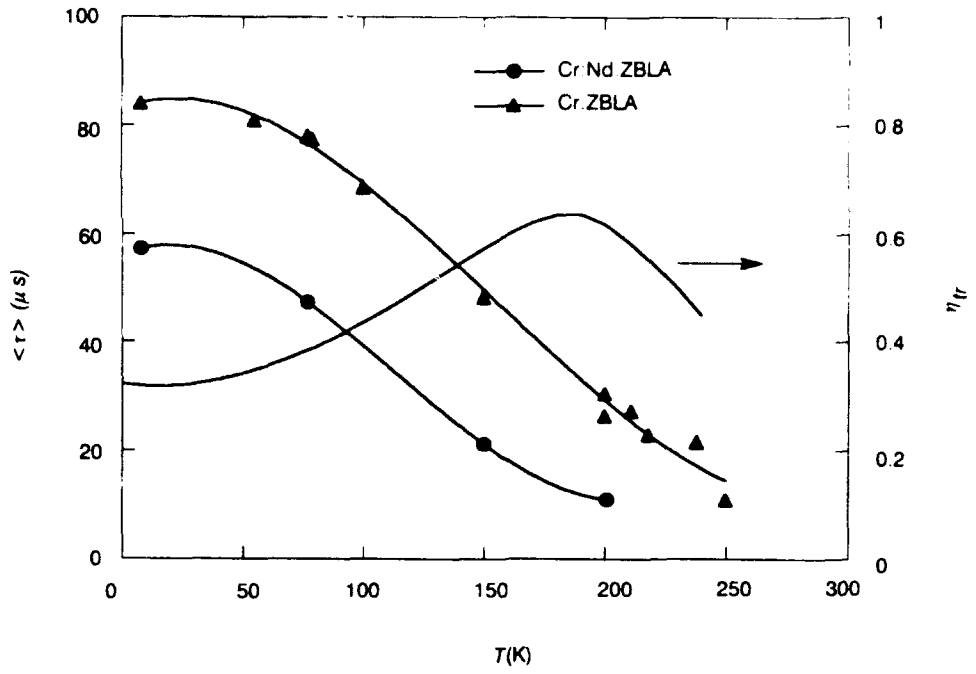

Figure 5. Fluorescence decay time constraints <τ> for the Cr^{3+} $^4T_2$ state as a function of temperature for Cr^{3+}:ZBLA and Cr^{3+}:Nd^{3+}:ZBLA. The calculated transfer efficiency is also shown.

SPECTRAL CHARACTERISTICS OF Cr^{3+}:Nd^{3+}:ZBLA

The absorption features of Nd^{3+}:ZBLA shown in figure 6 are relatively broad, typical of those in other glass host materials. Sharp crystal field split manifolds characteristic of crystalline host materials are generally absent in such glass hosts. The absorption spectra of the codoped sample is a superposition of the absorption from the Cr^{3+} and Nd^{3+} singly doped samples. From the measured integrated absorption bands, standard Judd-Ofelt theory [6,13] was used to calculate the intensity parameters, Ω_t, and the radiative transition probabilities. The measured and calculated oscillator strengths are listed in table 2. The quality of the fit is given by the rms deviation between theory and experiment, which is equal to 0.43×10^{-6}. Table 3 summarizes the values obtained for $\Omega_{2,4,6}$ and the calculated radiative transition probabilities and branching ratios for the $^4F_{3/2}$ transition to the ^4I_J states in Nd^{3+}:ZBLA glass. For comparison with the Nd^{3+}:ZBLA data, a similar analysis was carried out for Nd doped into LHG-8 glass and the crystalline materials $Y_3Al_5O_{12}$ and $Gd_3Sc_2Al_3O_{12}$. These results are included in table 3.

We measured the pulsed laser excited fluorescence of the codoped sample, with excitation into either the Cr^{3+} or Nd^{3+} absorption bands. For the spectra shown in figure 7, the excitation is at 670 nm in the Cr^{3+} absorption and the partial excitation transfer from Cr^{3+} to Nd^{3+} is evident from the combined fluorescence of both species. In figure 8, the excitation is at 580 nm, where the absorption is primarily due to Nd^{3+}, and the fluorescence is almost completely due to emission from Nd^{3+}.

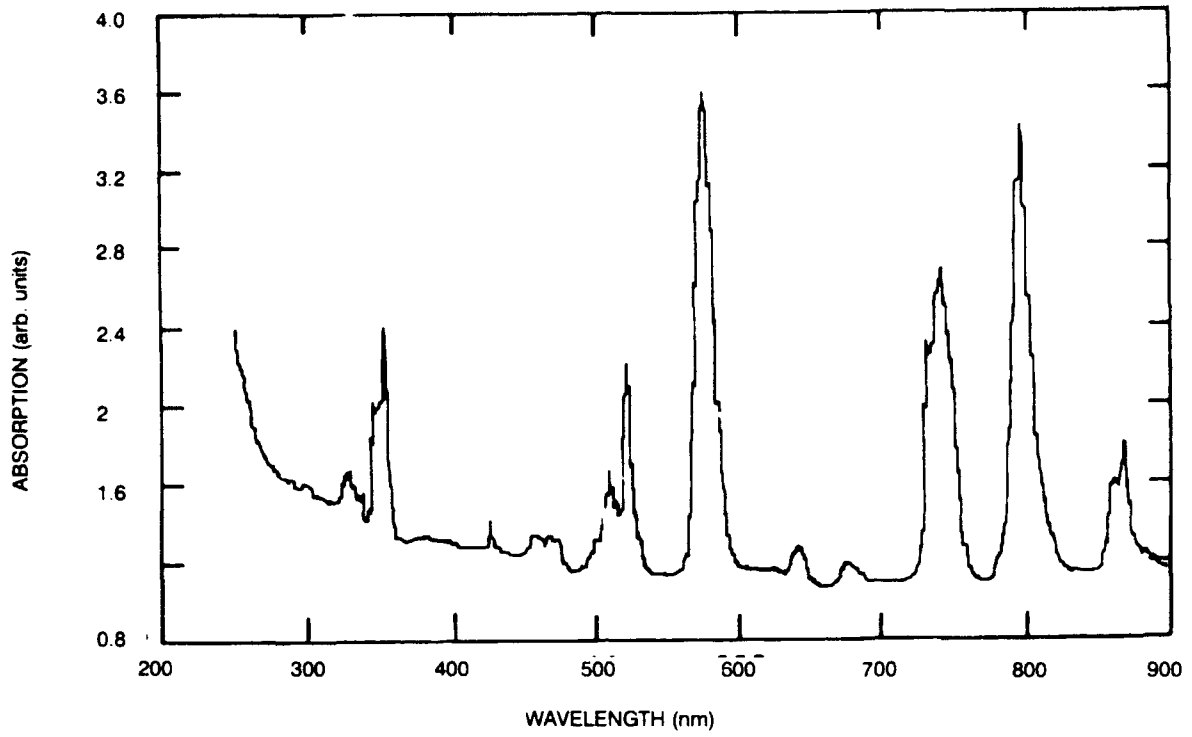

Figure 6. Absorption spectrum of Nd^{3+}:ZBLA glass.

Table 2. Oscillator strengths of Nd^{3+} ions in ZBLA.

Transition	λ (nm)	Measured (10^{-6})	Calculated (10^{-6})
$^4F_{3/2}$	868	0.84	1.32
$^4F_{5/2}$, $^2H_{9/2}$	797	3.53	3.61
$^4F_{7/2}$, $^2S_{3/2}$	741	3.48	3.47
$^4F_{9/2}$	682	0.26	0.28
$^2H_{11/2}$	635	0.40	0.10
$^4G_{5/2}$, $^2G_{7/2}$, $2K_{13/2}$	580	7.04	7.08
$^4G_{7/2}$, $^4G_{9/2}$	519	3.38	2.56
$^2K_{15/2}$, $^2G_{9/2}$, $(^2D, ^2P)_{3/2}$, $^4G_{11/2}$	471	0.90	0.67
$^2P_{1/2}$	432	0.16	0.35
$^4D_{3/2}$, $^4D_{5/2}$, $^2I_{11/2}$	354	3.98	3.58

Table 3. Nd^{3+} $^4F_{3/2}$ branching ratios, radiative lifetimes, and intensity parameters in ZBLA, LHG-8, $Y_3Al_5O_{12}$, and $Gd_3Sc_2Al_3O_{12}$.

Host	Branching Ratio				τ_{rad} (μs)	Intensity Parameter (10^{-20})		
	$^4I_{9/2}$	$^4I_{11/2}$	$^4I_{11/2}$	$^4I_{15/2}$		Ω_2	Ω_4	Ω_6
ZBLA	0.465	0.428	0.093	0.004	697	1.024	2.592	2.501
LHG-8	0.456	0.447	0.097	0.001	316	4.235	5.172	5.406
YAG	0.371	0.504	0.125	0.001	197	0.351	2.905	5.845
GSAG	0.415	0.474	0.110	0.001	275	0.132	2.622	3.706

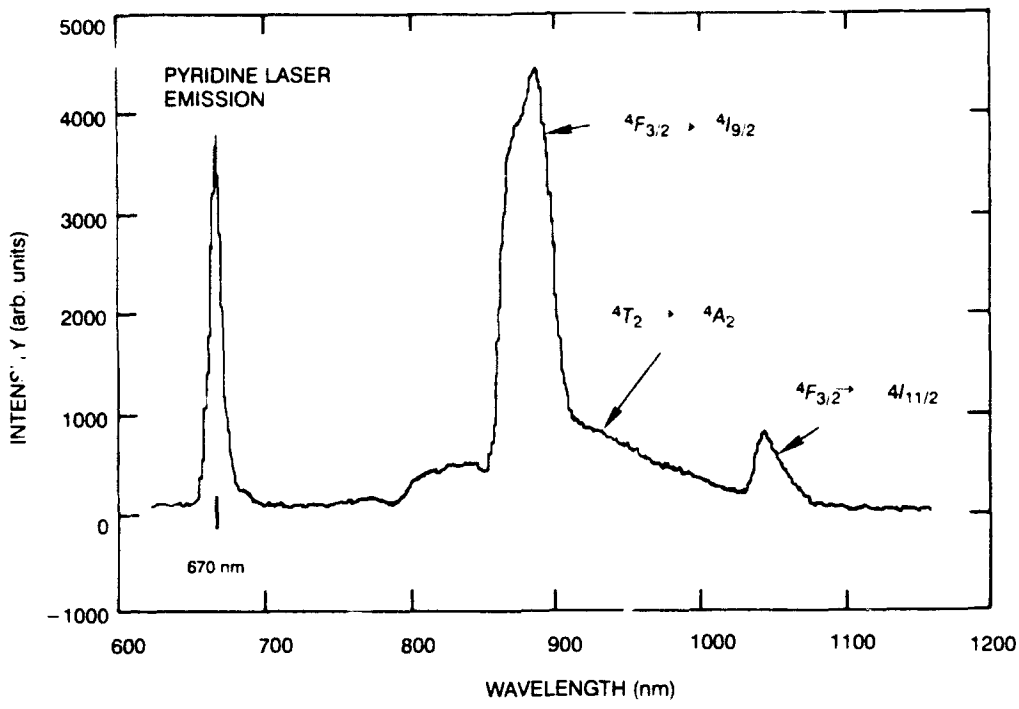

Figure 7. Fluorescence spectrum of Cr^{3+}:Nd^{3+}:ZBLA at 8 K with excitation in the Cr^{3+} absorption band at 670 nm. Emission from Nd^{3+} at 880 nm and 1.04 μm indicate energy transfer from Cr^{3+} to Nd^{3+}.

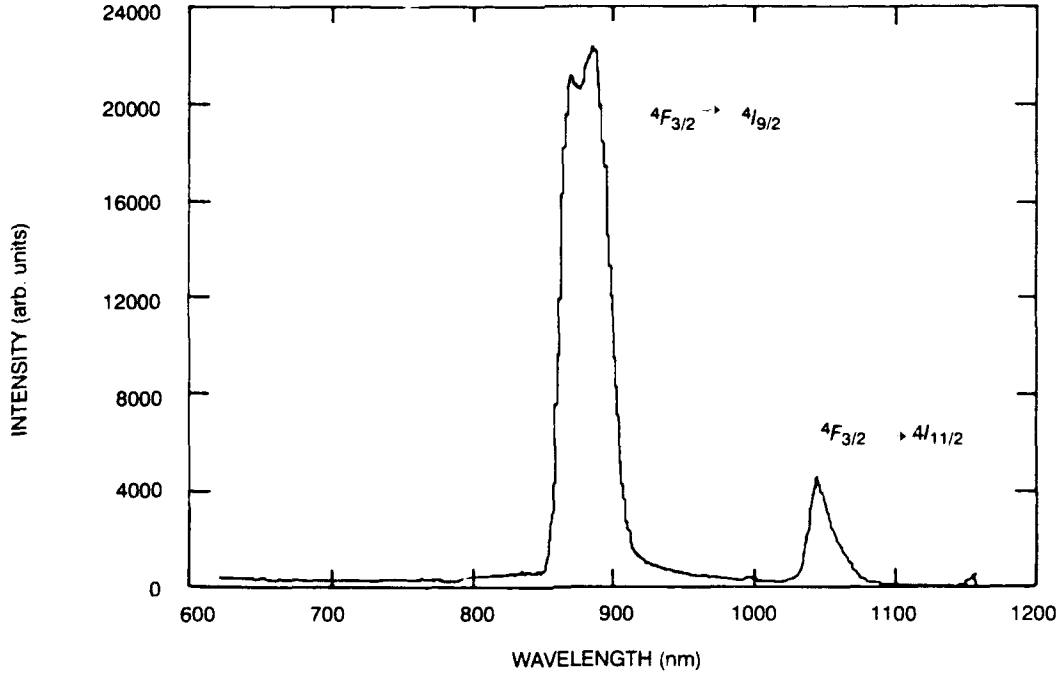

Figure 8. Fluorescence spectrum of Cr^{3+}:Nd^{3+}:ZBLA at 8 K with excitation in the Nd^{3+} absorption band at 580 nm. The weak Cr^{3+} emission is due to a small Cr^{3+} absorption at 580 nm.

Figure 9 shows the pertinent energy levels of Cr^{3+} and Nd^{3+} ions. The spectral overlap of the Cr^{3+} emission and the Nd^{3+} absorption is critical for the energy transfer from Cr^{3+} to Nd^{3+}. According to Dexter, the nonradiative energy transfer is due to the dipole–dipole interaction between the atoms. The rate W_{tr} for an isolated donor-acceptor pair separated by a distance R, is proportional to [14]

$$W_{tr} \sim \frac{1}{\tau_{rad} R^6} \int \frac{F_A(\nu) f_D(\nu)}{\nu^4} \, d\nu \tag{3}$$

where τ_{rad} is the effective radiative lifetime of the donor and $F_A(\nu)$ and $f_D(\nu)$ are the absorption and fluorescence line shapes of the acceptor and donor, respectively. Notice that the reverse energy transfer from Nd^{3+} to Cr^{3+} is not expected to occur and moreover would be an endothermic process.

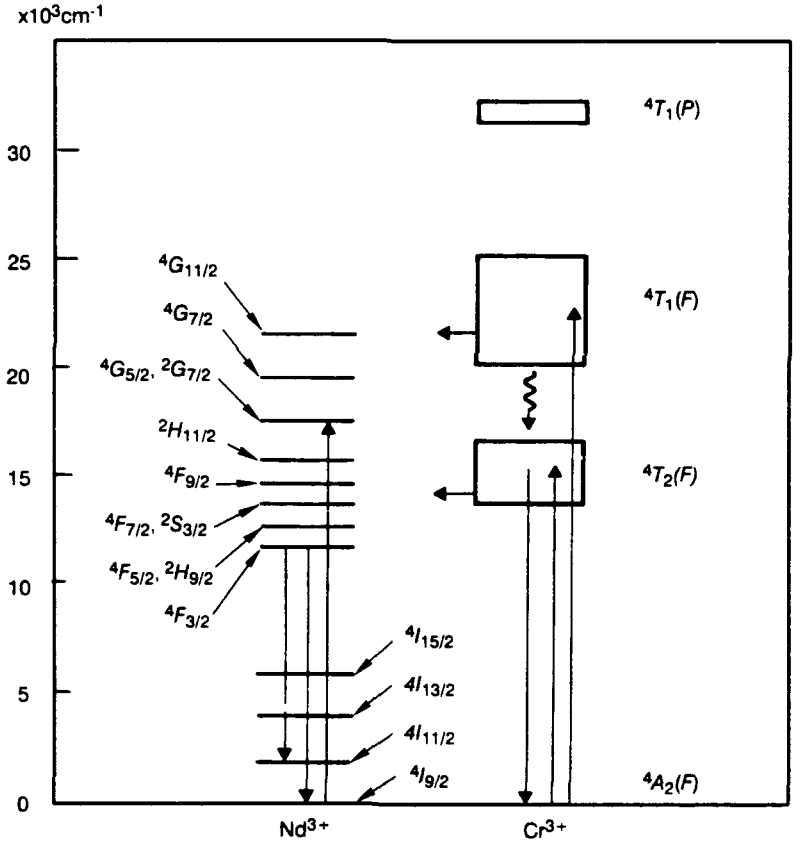

Figure 9. Energy levels of Nd^{3+} and Cr^{3+} in ZBLA glass.

Representative fluorescence decay curves from Cr^{3+}:Nd^{3+}:ZBLA at 8 and 77 K are given in figures 10 and 11. In both figures, curve a shows the selective excitation of Nd^{3+} at 580 nm and the exponential decay of the emission at 880 nm. There is a small decrease in the lifetime with increasing temperature indicating some nonradiative quenching. In curves b and c, the excitation is in the Cr^{3+} absorption band at 670 nm. In curve b, the Nd^{3+} and Cr^{3+} emissions at 880 nm

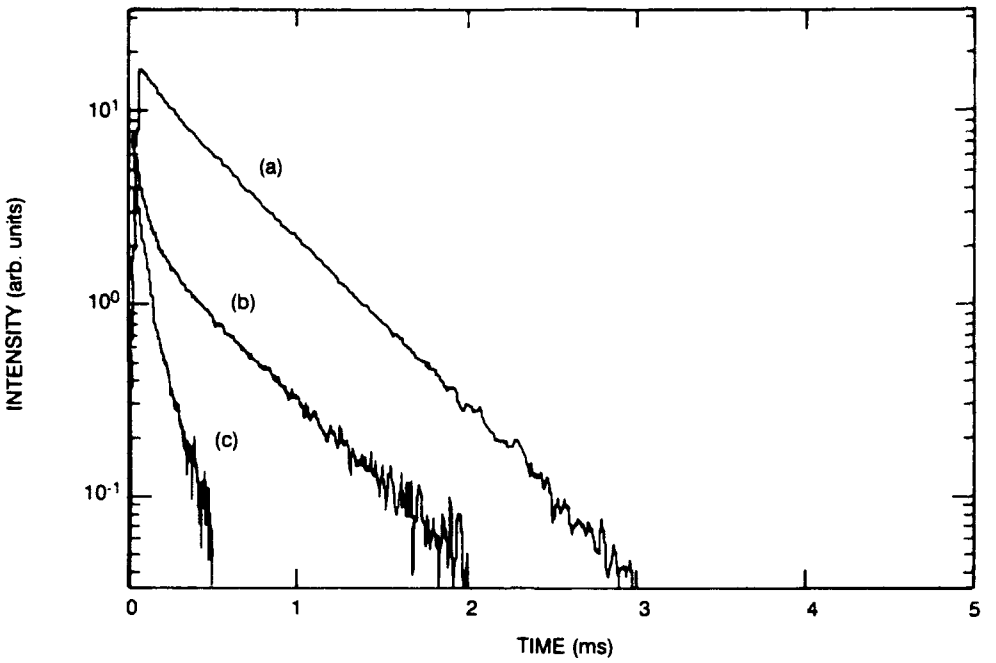

Figure 10. Fluorescence decay curves of Cr^{3+}:Nd^{3+}:ZBLA glass at 8 K: (a) Excitation at 580 nm and Nd^{3+} emission at 880 nm. (b) Excitation at 670 nm and combined Cr^{3+} and Nd^{3+} emission at 880 nm. (c) Excitation at 670 nm and Cr^{3+} emission at 940 nm.

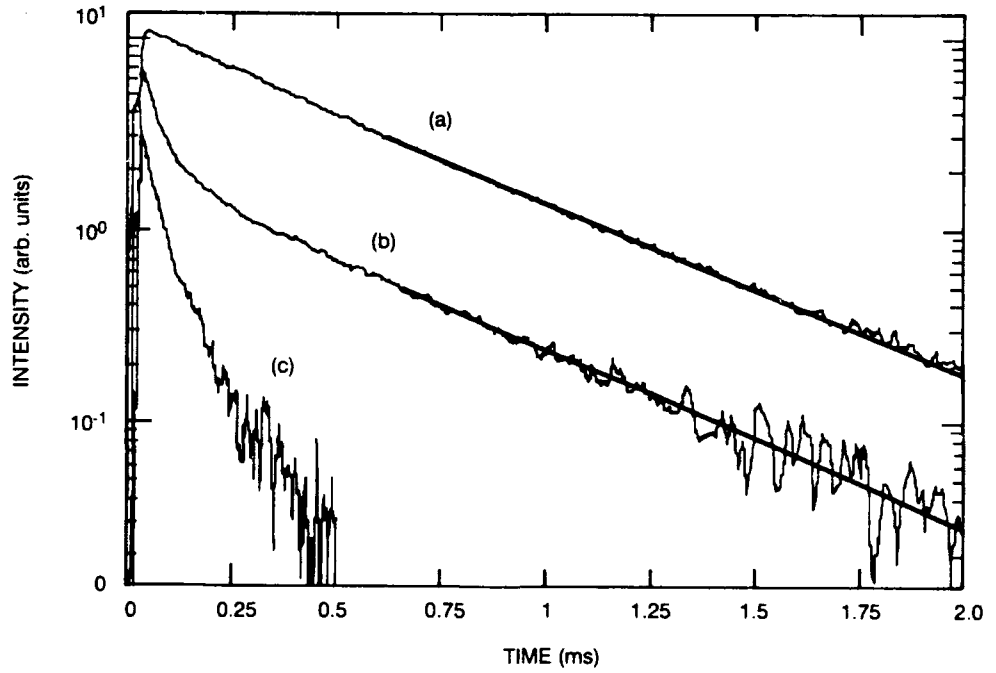

Figure 11. Fluorescence decay curves of Cr^{3+}:Nd^{3+}:ZBLA glass at 77 K: (a) Excitation at 580 nm and Nd^{3+} emission at 880 nm. (b) Excitation at 670 nm and combined Cr^{3+} and Nd^{3+} emission at 880 nm. (c) Excitation at 670 nm and Cr^{3+} emission at 940 nm.

overlap. The decay curves contain two components, a rapid initial decay due to the Cr^{3+} relaxation followed by a long decay representative of the Nd^{3+} decay. Curve c shows the decay of the broadband Cr^{3+} emission at 940 nm.

The temperature dependence of the Cr^{3+} $^4T_2$ lifetimes for both the codoped and singly doped samples are shown in figure 5. Again we note the strong quenching with increasing temperature. The significant result from these data is that at all temperatures where measurements were made, the presence of Nd^{3+} further increases the quenching of the Cr^{3+} fluorescence. We infer that this is due to an excitation transfer from Cr^{3+} to Nd^{3+}, consistent with the emission spectra. Assuming that the presence of Nd^{3+} does not affect other nonradiative decay mechanisms, the transfer rate W_{tr} is given approximately by

$$W_{tr} = 1/\tau_{(Cr,Nd)} - 1/\tau_{(cr)} \tag{4}$$

where the subscripts represent codoped and singly doped samples [14]. The transfer efficiency η_{tr} represents the quantum fraction of Cr^{3+} excitation that is transferred to Nd^{3+}, and is given by

$$\eta_{tr} = W_{tr}\tau_{(Cr,Nd)} = 1 - \tau_{(Cr,Nd)}/\tau_{(Cr)} \tag{5}$$

These expressions also assume first order kinetics or exponential decay, so that a single time constant is characteristic of the decay. We have calculated η_{tr} by using the averaged lifetime $<\tau>$ defined above. The lifetime data were fitted with simple polynomial functions and these were used in equation 5. The result is plotted in figure 5 also. At low temperatures, η_{tr} is ~0.4 and increases to ~0.6 at 200 K. It is not clear what happens at higher temperatures, since measurements were not made. These results are somewhat surprising, since the spectral overlap responsible for the dipole–dipole interaction in equation 3 should not change appreciably with temperature. The radiative decay rate is also expected to be insensitive to temperature. However, the nonradiative quenching clearly increases with temperature and should decrease η_{tr} as well as the fluorescence efficiency. More careful measurements at higher temperatures and the direct monitoring of the Nd^{3+} emission after Cr^{3+} excitation would help clarify this issue.

CONCLUSIONS

In this report, we have described the spectroscopic features of Cr^{3+} and of codoped Cr^{3+} and Nd^{3+} in ZBLA glasses. For Cr^{3+} in an octahedral site symmetry, the lower energy levels were assigned with the help of the Tanabe-Sugano diagrams. The complex structure in the absorption spectrum at 670 nm is due to the near coincidence of the $^2T_1$ and ^2E states superimposed on the broad $^4T_2$ state of Cr^{3+}. Excitation of the $^4T_2$ state leads to a broad, Stokes-shifted fluorescence band from 750 nm to 1100 nm, similar to the emission of Cr^{3+} in the phosphate glasses [7]. This emission overlaps the Nd^{3+} absorption bands in this material and leads to nonradiative energy transfer from Cr^{3+} to Nd^{3+}. We have measured quantum transfer efficiencies in the range of 0.4 to 0.6 from low temperatures up to 200K. These results are similar to values obtained by Reisfeld, et al., in their study of the transfer from Mn^{2+} to Nd^{3+} in fluoride glasses with composition 35 PbF_2, 24MnF_2, 35GaF_3, AlF_3, (4–x)LaF_3, $x$$NdF_3$, and x = 0.2 and 2.0 [4]. The fluorescence was found to be strongly quenched with increasing temperature. It is not clear if the excitation transfer efficiency decreases at higher temperatures, although this is expected.

REFERENCES

1. B. Bendow, "Mid-Infrared Fiber Optics Technology (A Study and Assessment)," Naval Ocean Systems Center, San Diego, CA, Contract Report 243, Feb. 1984.

2. Y. Ohishi, S. Mitachi, T. Kanamori, and T. Manabe, Phys. Chem. Glasses, 24 (1983)135; P. W. France, S. F. Carter, M. W. Moore, J. R. Williams, Electron. Lett. 21 (1985) 602; G. Fuxi and L. Huimin, J. Non-Cryst. Solids, 80 (1986)20.

3. Y. Tanabe and S. Sugano, J. Phys. Soc. (Japan), 9 (1954)766.

4. J. Lucas, M. Chanthanasinh, M. Poulain, M. Poulain, P. Brun, and M. J. Weber, J. Non-Cryst. Solids, 27 (1978)273; R. Reisfeld, G. Katz, N. Spector, C. K. Jorgensen, C. Jacoboni, and R. Depape, J. Solid State Chem. 41 (1982)253; R. Reisfeld, G. Katz, C. Jacoboni, R. Depape, M. G. Drexhage, R. N. Brown, and C. K. Jorgensen, J. Solid State Chem. 48 (1983)323; R. Reisfeld, E. Greenberg, R. N. Brown, M. G. Drexhage, and C. K. Jorgensen, Chem. Phys. Lett. 95 (1983); M. D. Shinn, W. A. Sibley, M. G. Drexhage, and R. N. Brown, Phys. Rev. B24 (1983)6635; K. Tanimura, M. D. Shinn, W. A. Sibley, M. G. Drexhage, and R. N. Brown, Phys. Rev. 30B (1984)2429; M. Eyal, E. Greenberg, R. Reisfeld, and N. Spector, Chem. Phys. Lett. 117 (1985)108; R. Reisfeld, M. Eyal, E. Greenberg, and C. K. Jorgensen, Chem. Phys. Lett. 118 (1985); R. Reisfeld and M. Eyal, Heavy Metal Fluoride Glasses, AFWL-TR 86-37, April, 1987.

5. J. Murphy, R. C. Ohlmann and R. Mazelsky, Phys. Rev. Lett. 13 (1964)135; M. J. Taylor, Proc. Phys. Soc. 90 (1967)487; A. G. Avanesov, Y. K. Voron'ko, B. I. Denker, A. A. Kut'enkev, G. V. Maksimova, V. V. Osiko, E. I. Sidorova, Y. P. Timofeev, and I. A. Shcherbakov, Sov. J. Quantum Electron. 9(10) (1979)1323; D. Pruss, G. Huber, A. Beimowski, V. V. Laptev, I. A. Shcherbakow, and Y. V. Zharikov, Appl. Phys. B28 (1982)355; V. G. Ostroumov, Y. S. Privis, V. A. Smirnov, and I. A. Shcherbakov, J. Opt. Soc. Am. B3 (1986)81; R. Reisfeld and A. Kisilev, 9Chem. Phys. Lett. 1115 (1985)457.

6. B. R. Judd, Phys. Rev. 127 (1962)750; G. S. Ofelt, J. Chem. Phys. 37 (1962)511.

7. R. E. Tischer and L. Helmholz, J. Chem. Phys. 48 (1968)4291; S. A. Brawer and W. B. White, J. Chem. Phys., 64(1977)2043; E. J. Sharp, J. E. Miller and M. J. Weber, Phys. Lett. 30A(1969)142; L. J. Andrews, A. Lempicki and B. C. McCollum, J. Chem. Phys. 74(1981)5526; L. J. Andrews, G. H. Beall and A. Lempicki, J. Lumin. 36(1986)65; A. J. Wojtowicz and A. Lempicki, J. Lumin. 39(1988)189.

8. M. Wolfsberg and L. Helmholz, J. Chem. Phys. 20(1952)837; A. D. Liehr and C. J. Ballhausen, J. Mol. Spec. 2(1958)342.

9. A. Lempicki, L. J. Andrews, S. J. Nettel, and B. C. McCollum, Phys. Rev. Lett. 44(1980)1234.

10. M. D. Sturge, H. J. Guggenheim and M. H. L. Price, Phys. Rev. B2(1970)2459.

11. U. Fano, Phys. Rev. 124(1961)1866.

12. M. J. Weber, E. J. Sharp and J. E. Miller, J. Phys. Chem. Solids, 32(1971)2275.

13. W. T. Carnall, P. R. Fields and K. Rajnak, J. Chem. Phys. 49(1968)4412.

14. D. L. Dexter, J. Chem. Phys. 21(1953)836.

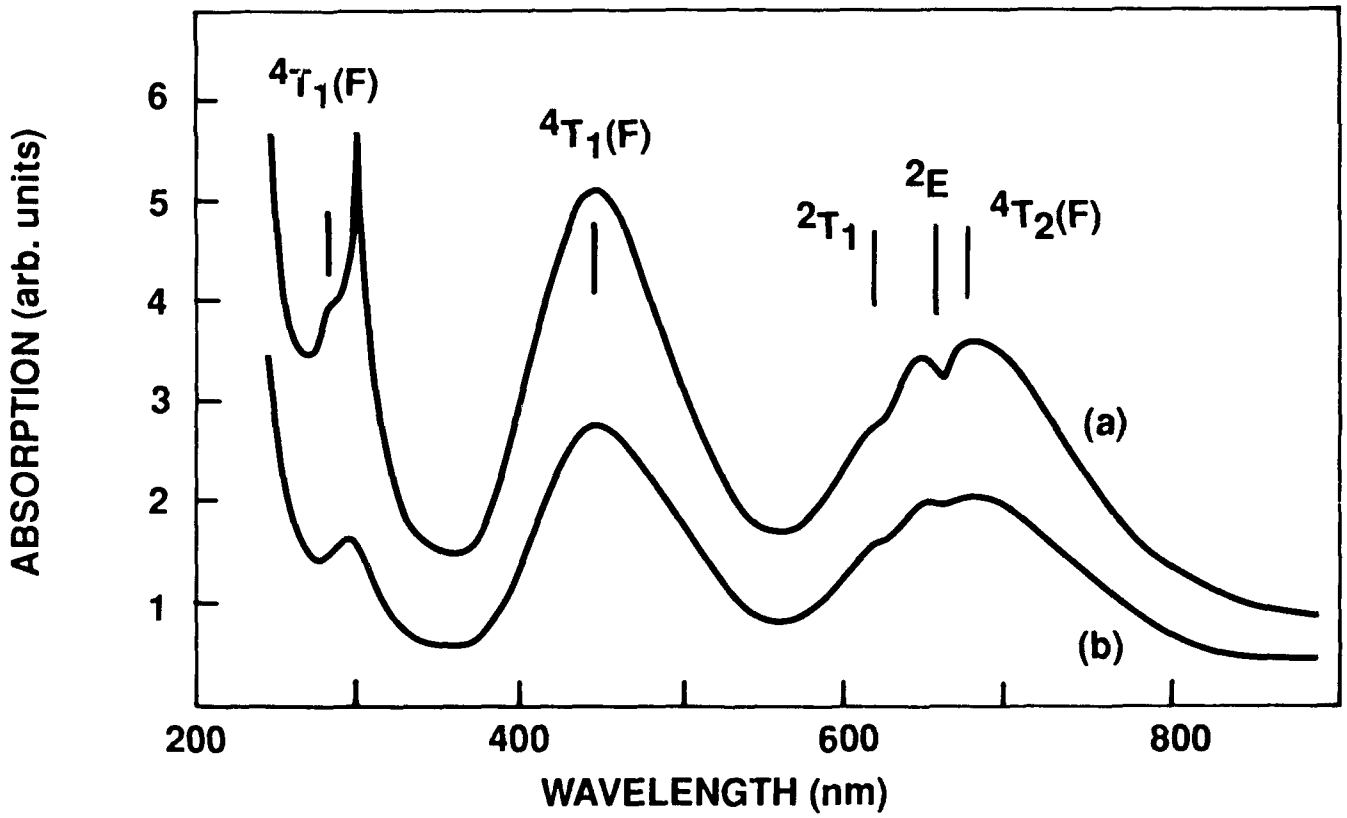

Figure 1. (a) Absorption spectrum of Cr(III) in ZBLA glass at 8°K.
(b) Room temperature absorption spectrum of Cr(III) in ZBLA glass.

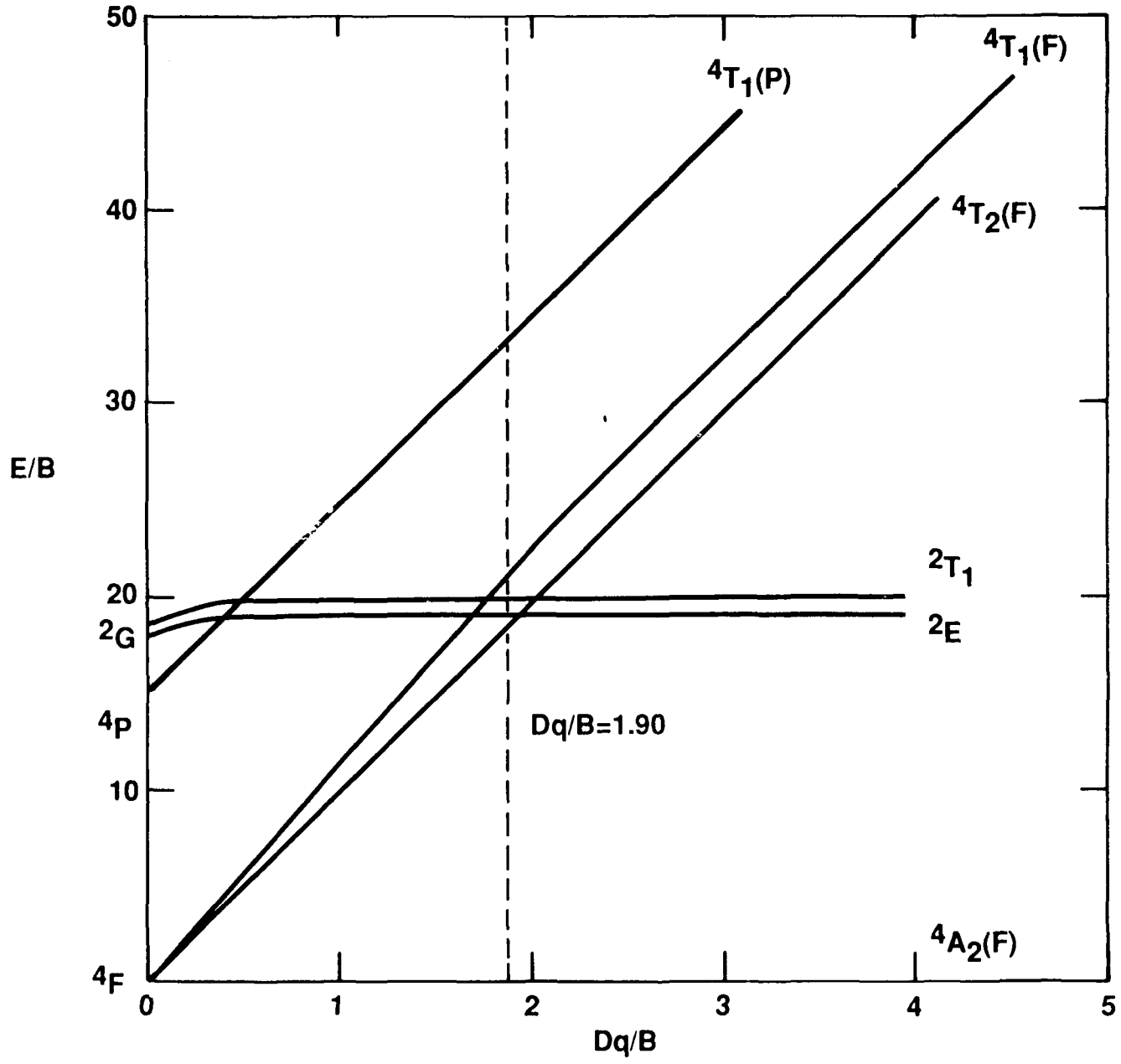

Figure 2. Lower energy levels vs. crystal field strength in units of the Racah-parameter B for octahedrally coordinated Cr(III).

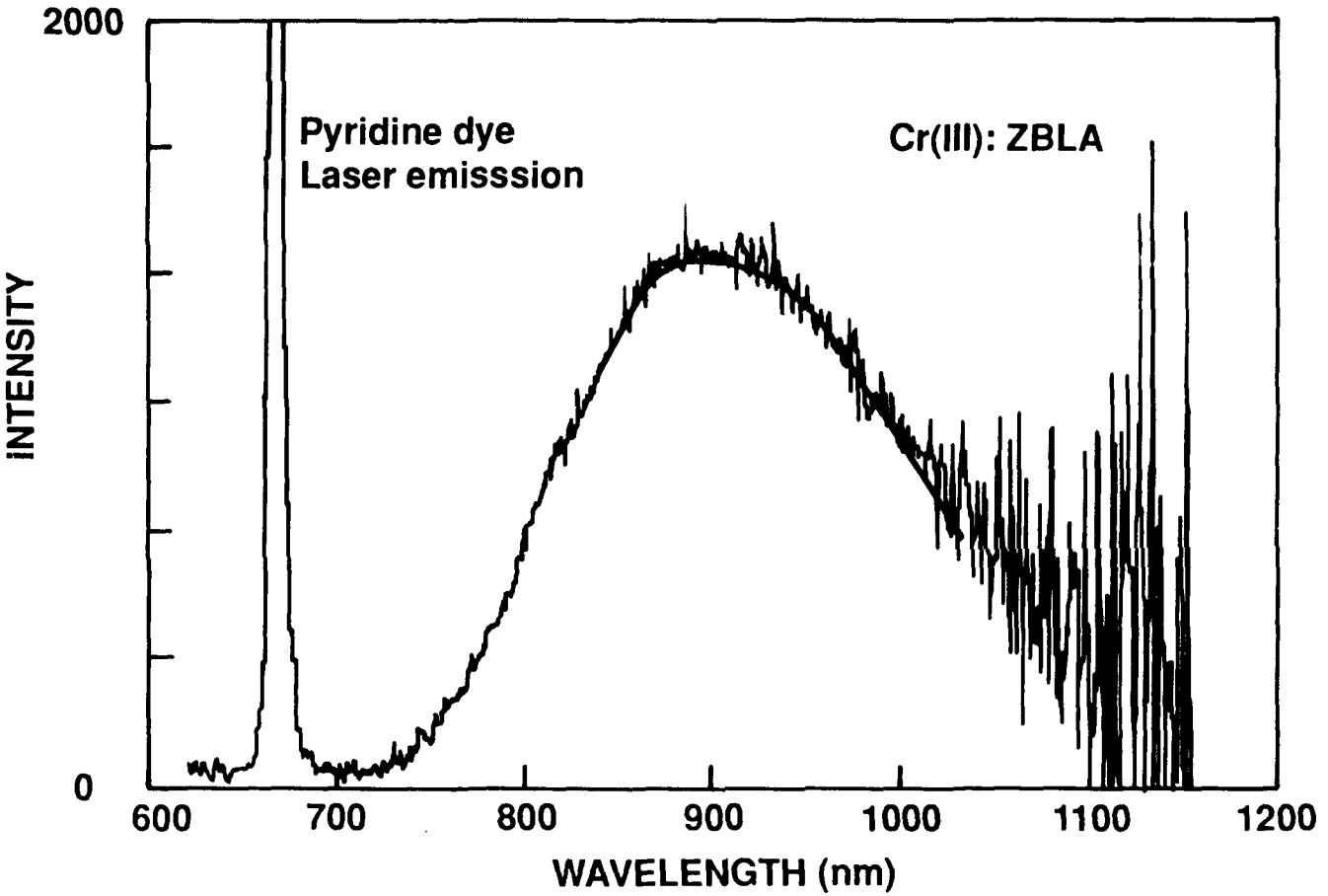

Figure 3. Laser excited fluorescence of Cr(III) in ZBLA at 8 K; excitation at 670 nm, broadband emission at ~ 900 nm.

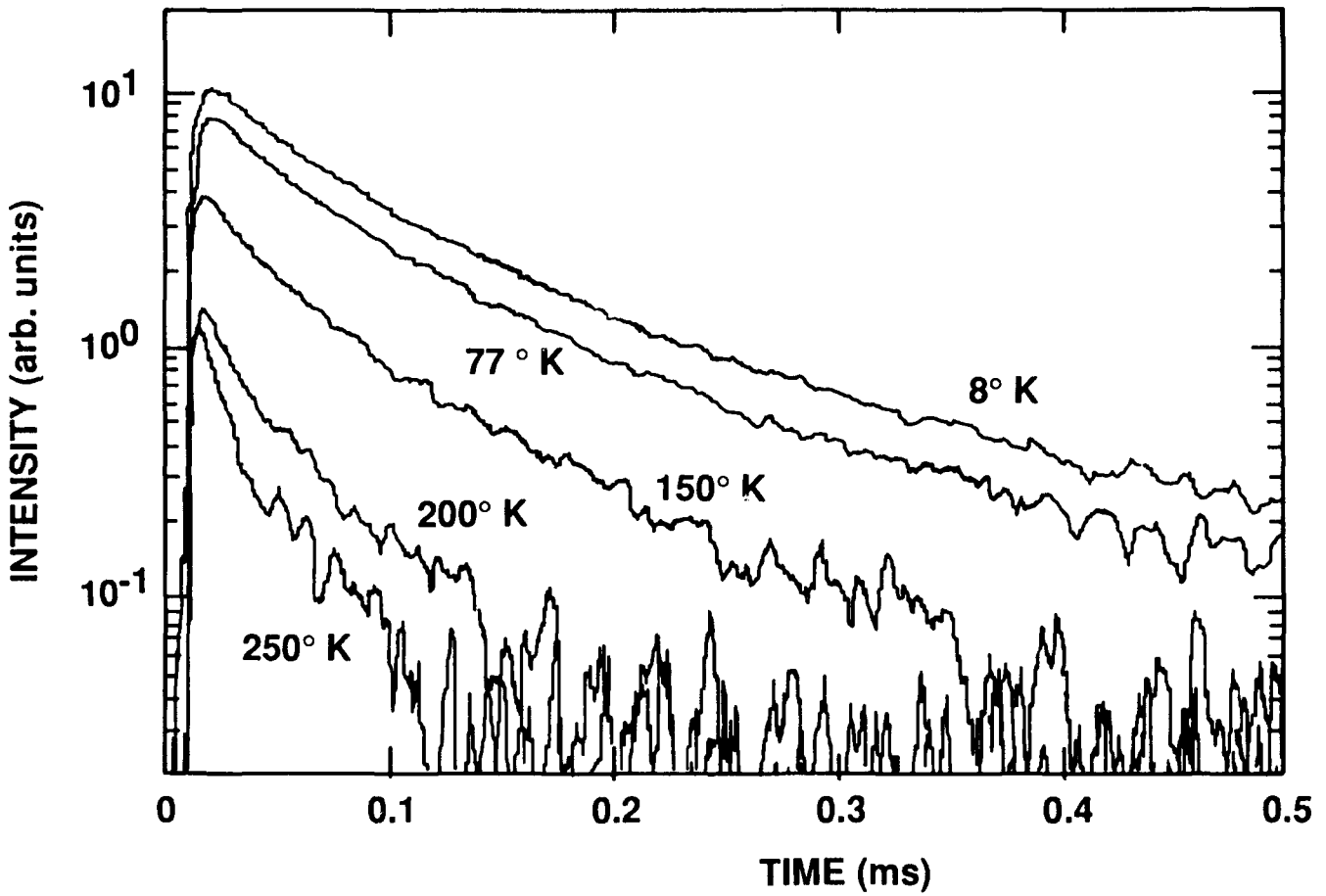

Figure 4. Luminescent decay curves of Cr (III) in ZBLA glass, excitation at 670 nm, emission at 900 nm.

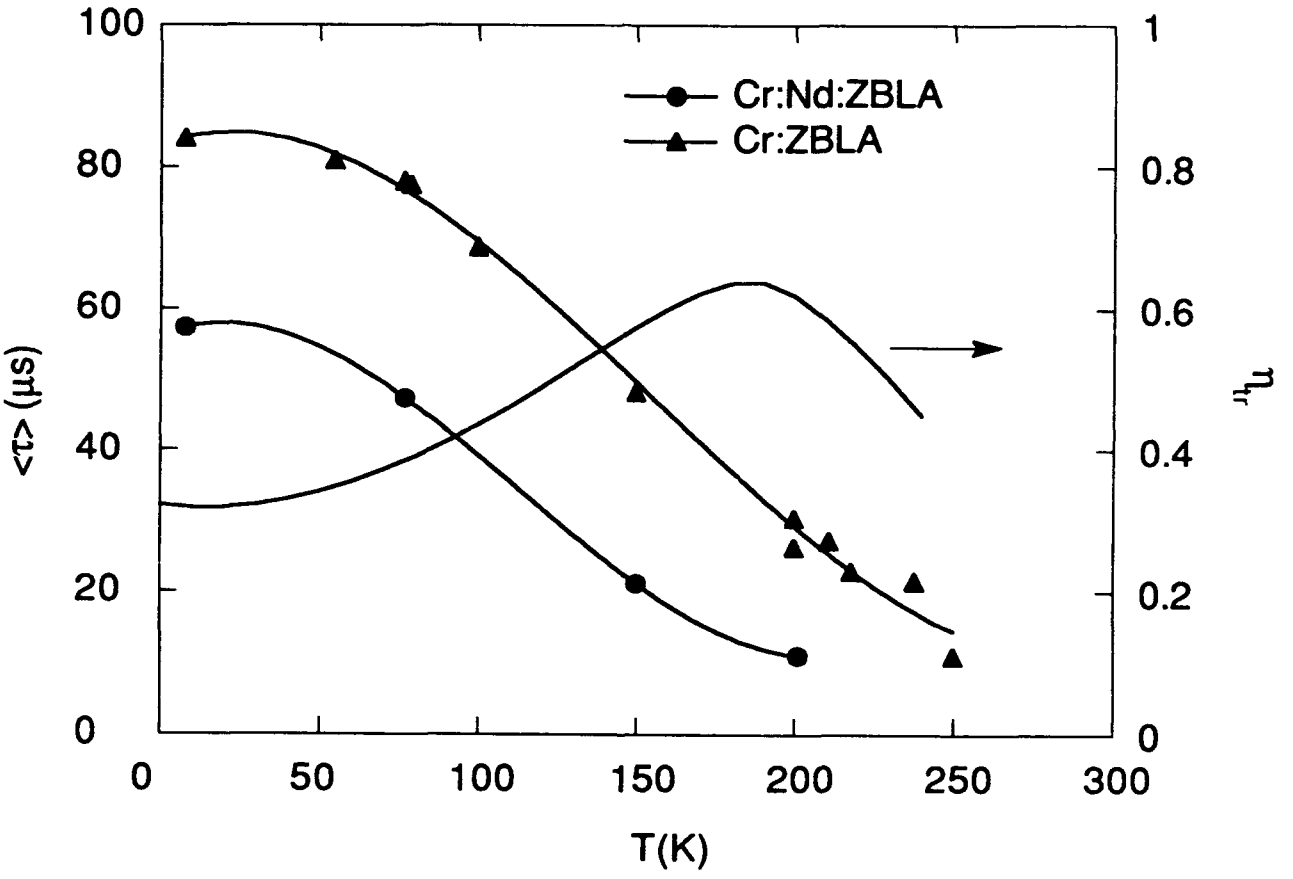
100
80
60
40
20
0
1
0.8
0.6
0.4
0.2
0
0
50
100
150
200
250
300
T(K)
<τ> (μs)
η
Cr:Nd:ZBLA
Cr:ZBLA

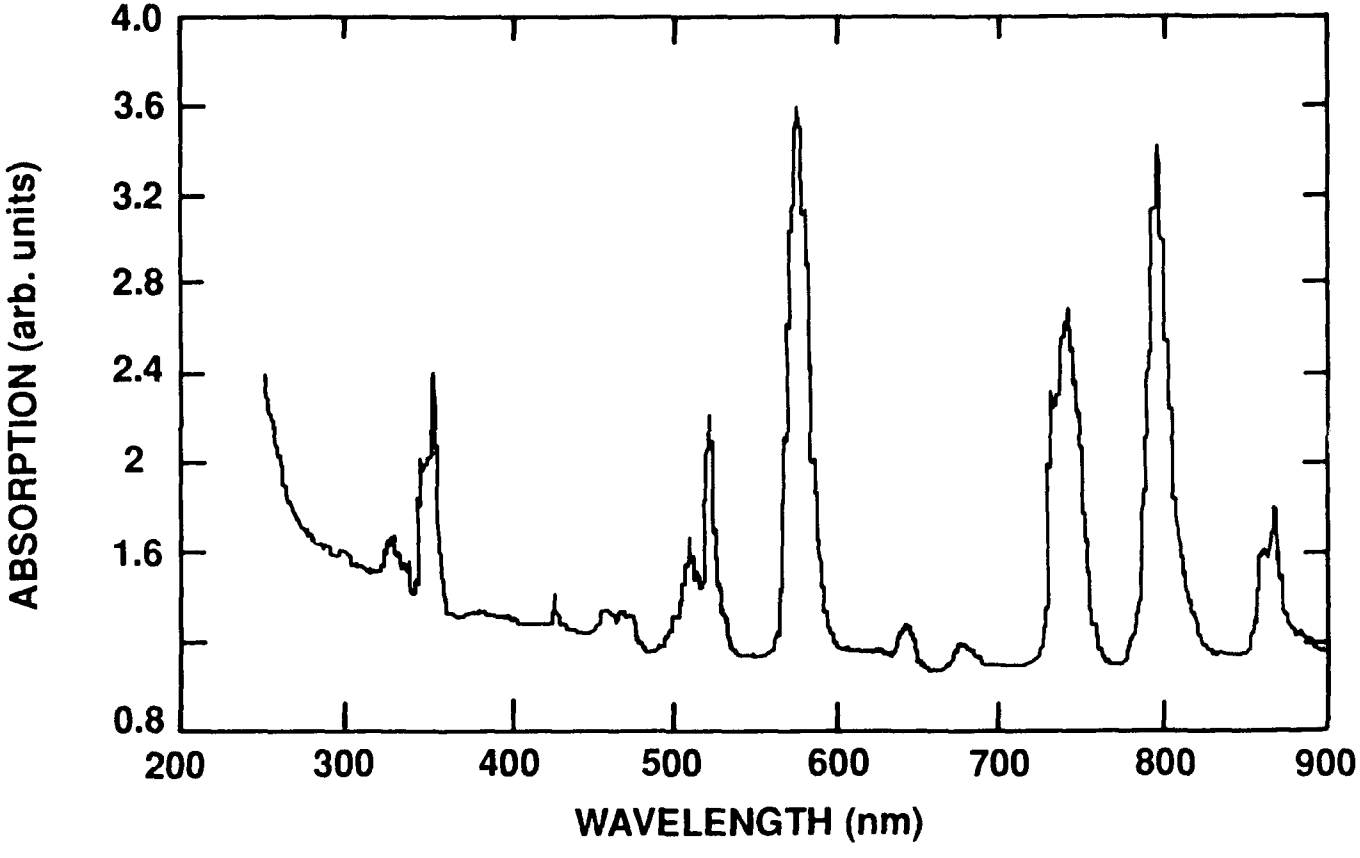

Figure 6. Absorption spectrum of Nd (III) in ZBLA glass.

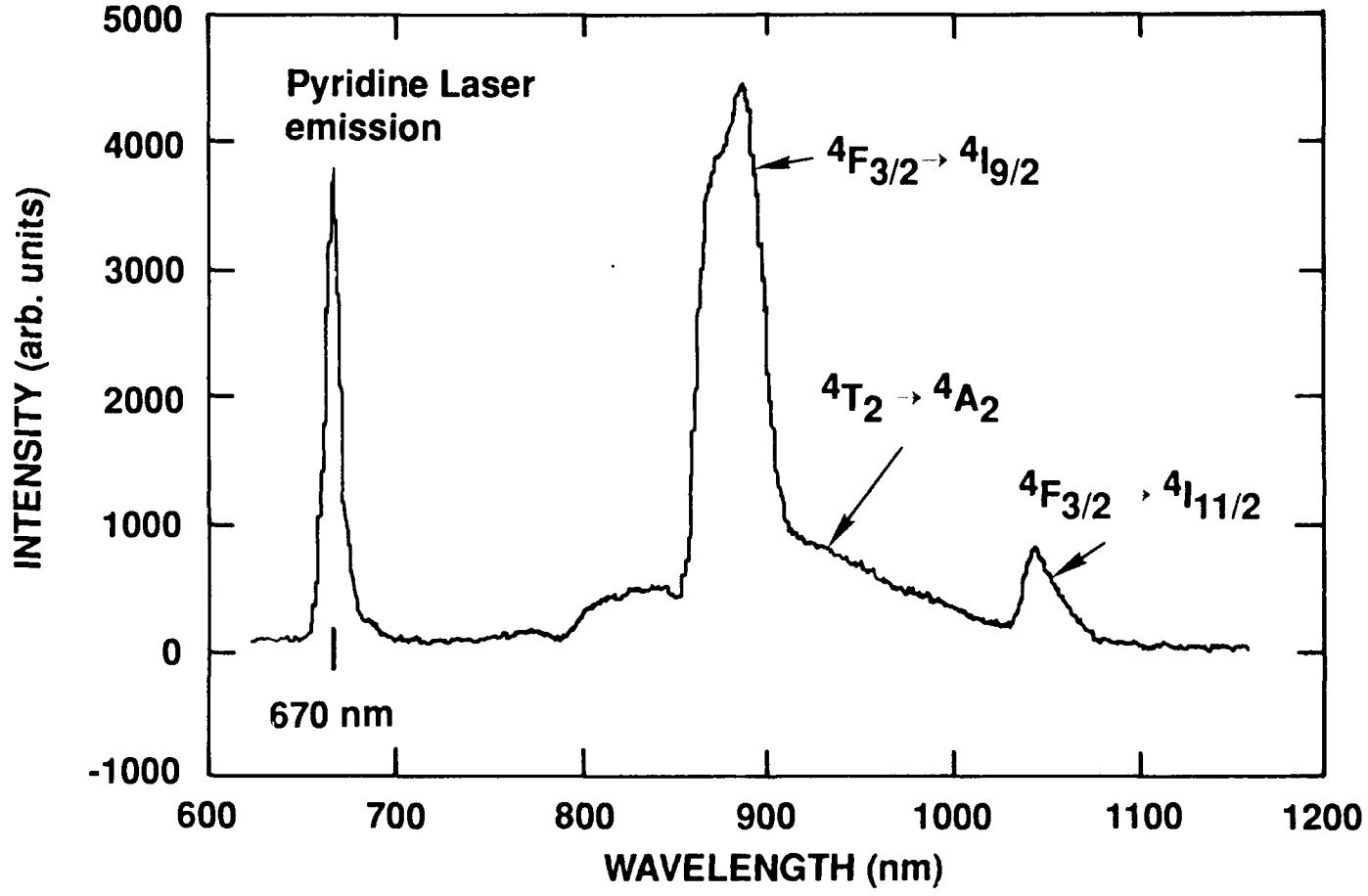

Figure 7. Laser excited fluorescence of Nd(III): Cr(III) in ZBLA at 8°K. Excitation at 670 nm, emission at 880 nm and 1.04 μm correspond to the $^4F_{3/2} \rightarrow {}^4I_{9/2}$, $^4I_{11/2}$ Transitions of Nd(III). The broadband emission at 940 nm is due to $^4T_2(F) \rightarrow {}^4A_2(F)$ transition of Cr(III).

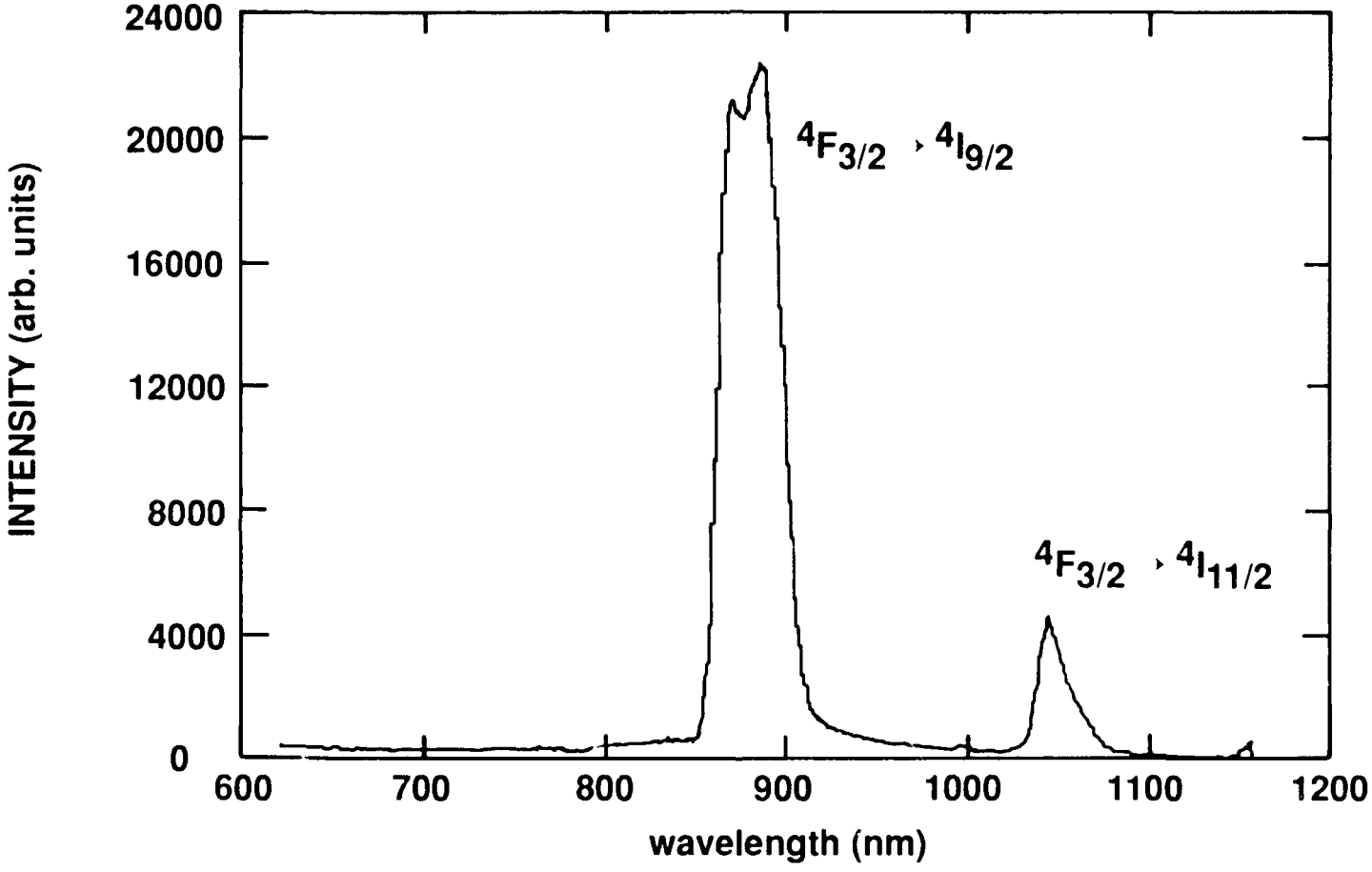

Figure 8. Laser excited fluorescence of Nd(III); Cr(III) in ZBLA glass at 8°K. Excitation at 580 nm. The emissions at 880 nm and 1.04 μm correspond to the $^4F_{3/2}$ › $^4I_{9/2}$, and $^4I_{11/2}$ transitions respectively.

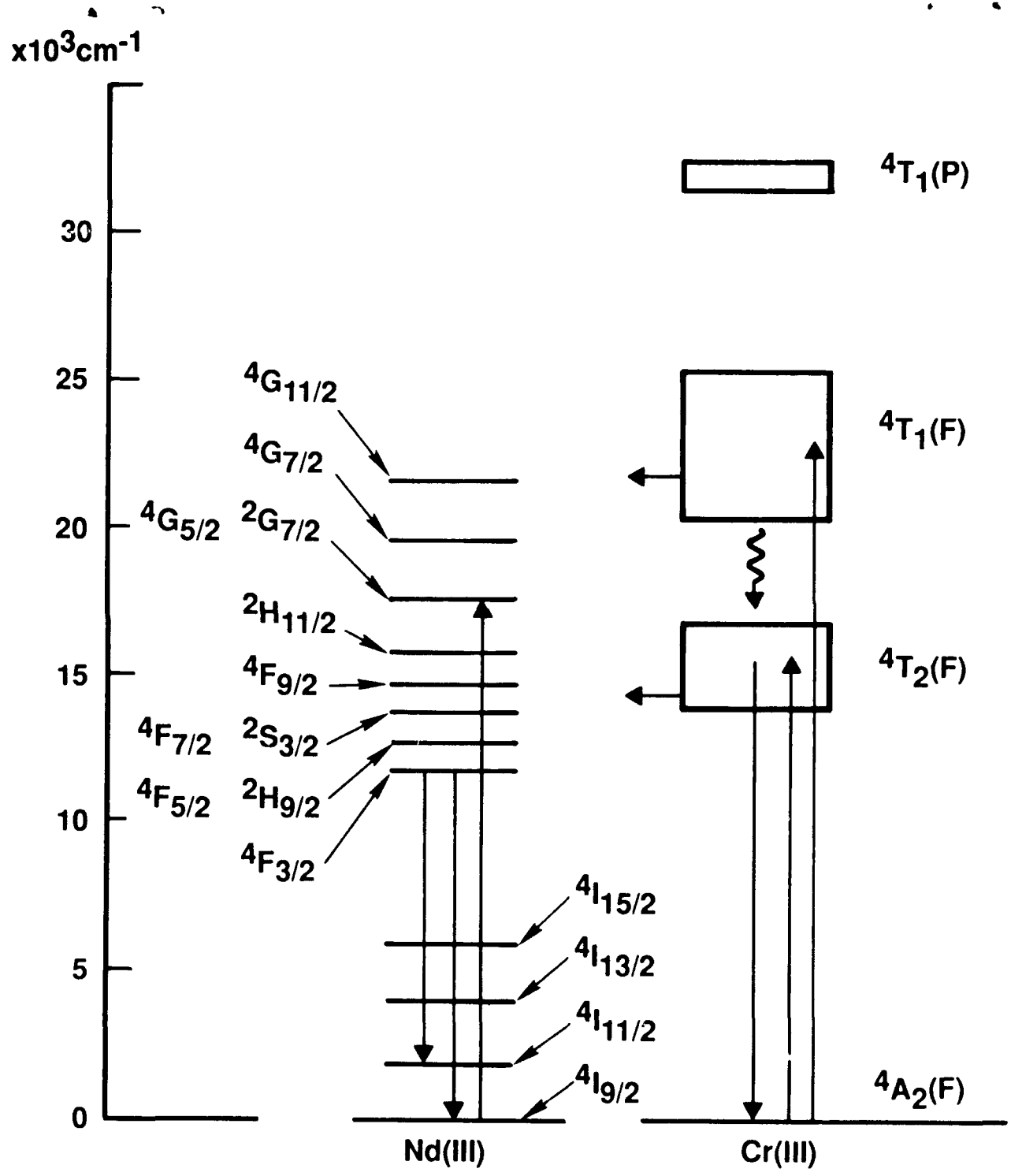

Figure 9. Scheme of energy levels of Nd (III) and Cr (III) in ZBLA glass.

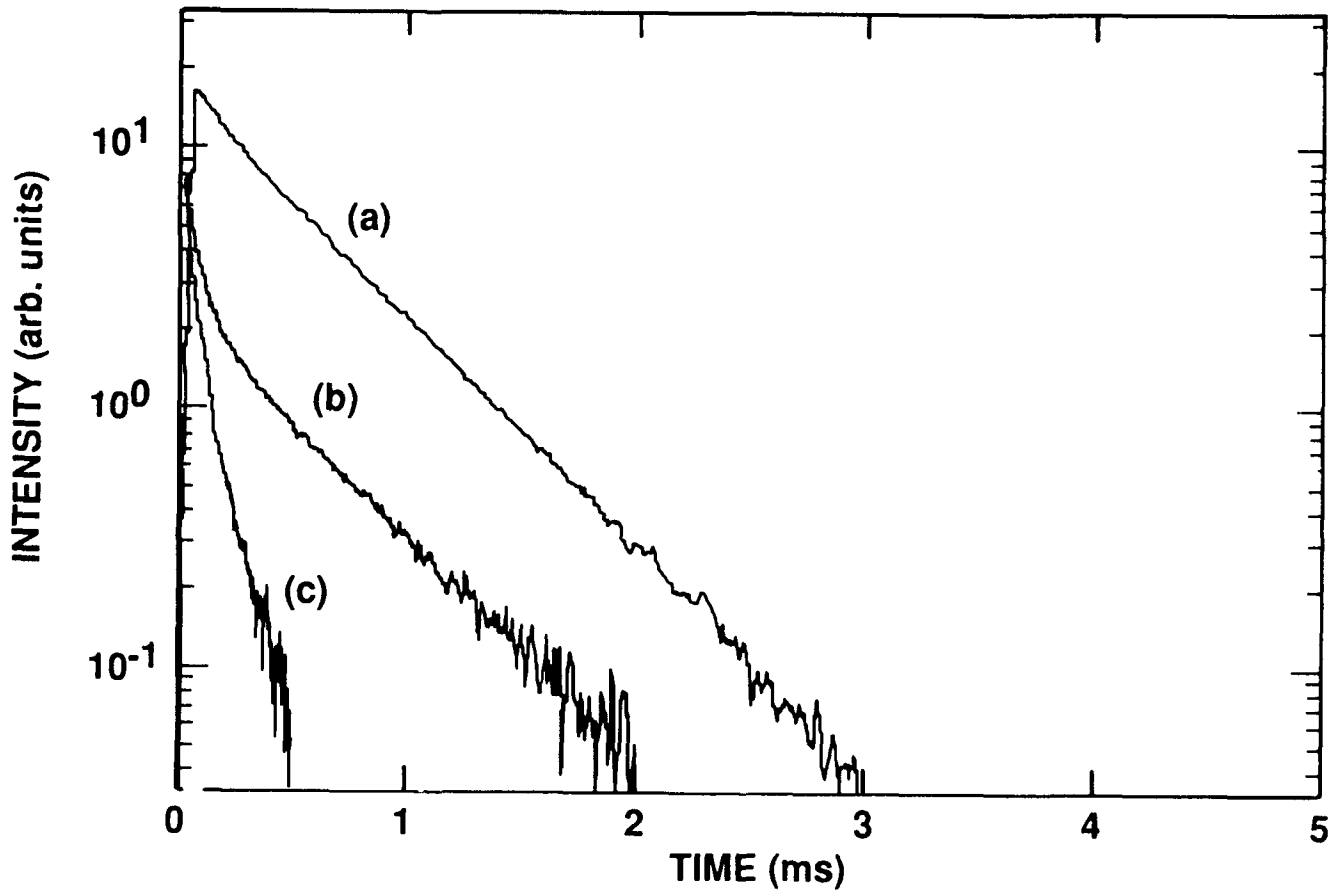

Figure 10. Luminescent decay curves of Nd(III)Cr(III):ZBLA glass at 8°K.
(a) Excitation at 580 nm, Nd(III) emission at 880 nm,
lifetine τ_{in} =473 μs.
(b) Excitation at 670 nm, Nd(III) emission at 880 nm,
lifetime τ_{in} =378 μs.
(c) Exitation at 670 nm, Cr(III) Emission at 940 nm,
lifetime τ_{in} =84 μs.

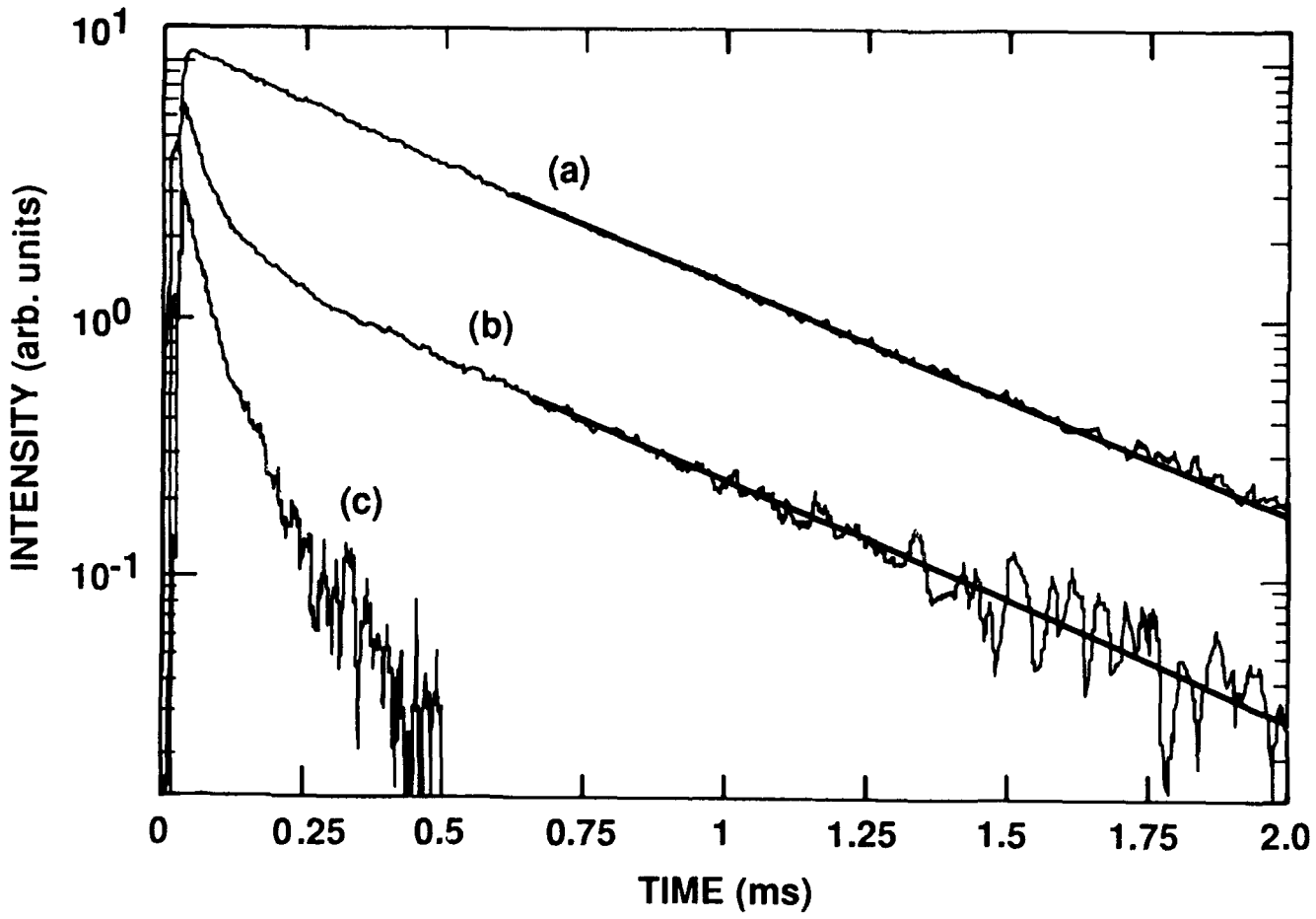

Figure 11. Luminescent decay curves of Nd (III)Cr(III): ZBLA glass at 77°K.
(a) Excitation at 580 nm; emissionat 880 nm, lifetime τ_{in} =438 μs.
(b) Excitation at 670 nm, emission at 880 nm, lifetime τ_{in}=359 μs.
(c) Excitation at 640 nm, emission at 940 nm, lifetime τ_{in}=69 μs.

REPORT DOCUMENTATION PAGE

Form Approved
OMB No 0704-0188

1 AGENCY USE ONLY *(Leave blank)*	2 REPORT DATE	3 REPORT TYPE AND DATES COVERED
	August 1993	Final: Oct 1987 – Sep 1988

4 TITLE AND SUBTITLE

OPTICAL PROPERTIES OF CHROMIUM AND NEODYMIUM IN ZIRCONIUM-BARIUM-LANTHANUM-ALUMINUM FLUORIDE GLASS

5 FUNDING NUMBERS

84-ZT99
DN308063

6 AUTHOR(S)

F. E. Hanson and H. H. Caspers

7 PERFORMING ORGANIZATION NAME(S) AND ADDRESS(ES)

Naval Command, Control and Ocean Surveillance Center (NCCOSC)
RDT&E Division
San Diego, CA 92152-5732

8 PERFORMING ORGANIZATION REPORT NUMBER

TR 1623

9 SPONSORING/MONITORING AGENCY NAME(S) AND ADDRESS(ES)

Office of Chief of Naval Research
Independent Research Programs (IR)
OCNR-10P
Arlington, VA 22217-5000

10 SPONSORING/MONITORING AGENCY REPORT NUMBER

11. SUPPLEMENTARY NOTES

12a. DISTRIBUTION/AVAILABILITY STATEMENT

Approved for public release; distribution is unlimited.

12b DISTRIBUTION CODE

13. ABSTRACT *(Maximum 200 words)*

The optical properties are reported of chromium and neodymium doped in zirconium-barium-lanthanum-aluminum fluoride glass (ZBLA). The fluorescence of Cr^{3+} and of co-doped Cr^{3+}, Nd^{3+} glasses is investigated. Fluroescence decay rates of Cr^{3+} and Nd^{3+} are measured at various temperatures, and the excitation transfer efficiency between Cr^{3+} and Nd^{3+} is determined. The absorption spectrum of Nd^{3+}:ZBLA is characterized in terms of the Judd-Ofelt model of crystal field-induced electric-dipole transitions. The three phenomenological intensity parameters for Nd^{3+} in ZBLA glass $\Omega_{2,4,6}$, are compared to those obtained for Nd^{3+} in $Y_3Al_5O_{12}$, $Gd_3Sc_2Al_3O_{12}$, and LHG-8 glass.

14. SUBJECT TERMS

chromium spectroscopy
laser materials
neodymium spectroscopy
energy transfer/heavy metal fluoride glass
fluorescence quenching

15 NUMBER OF PAGES

31

16 PRICE CODE

17 SECURITY CLASSIFICATION OF REPORT	18 SECURITY CLASSIFICATION OF THIS PAGE	19 SECURITY CLASSIFICATION OF ABSTRACT	20 LIMITATION OF ABSTRACT
UNCLASSIFIED	UNCLASSIFIED	UNCLASSIFIED	SAME AS REPORT

21a NAME OF RESPONSIBLE INDIVIDUAL	21b TELEPHONE *(include Area Code)*	21c OFFICE SYMBOL
F. E. Hanson	(619) 553-5720	Code 843

INITIAL DISTRIBUTION

Code 0012	Patent Counsel	(1)
Code 0141	A. Gordon	(1)
Code 02712	Archive/Stock	(6)
Code 0274B	Library	(2)
Code 55	H. E. Rast	(1)
Code 80	R. J. Kochanski	(1)
Code 804	E. Schimitischek	(1)
Code 804	G. W. Beaghler	(1)
Code 84	C. E. Gibbens	(1)
Code 843	D. M. Gookin	(1)
Code 843	F. E. Hanson	(6)

Defense Technical Information Center
Alexandria, VA 22304–6145 (4)

NCCOSC Washington Liaison Office
Washington, DC 20363–5100

Center for Naval Analyses
Alexandria, VA 22302–0268

Navy Acquisition, Research and Development
Information Center (NARDIC)
Washington, DC 20360–5000

GIDEP Operations Center
Corona, CA 91718–8000

NCCOSC Division Detachment
Warminster, PA 18974–5000